THE JOURNAL OF BIOLOGICAL CHEMISTRY VOL. 288, NO. 3, pp. 1907–1917, January 18, 2013
© 2013 by The American Society for Biochemistry and Molecular Biology, Inc. Published in the U.S.A.

# Versican Processing by a Disintegrin-like and Metalloproteinase Domain with Thrombospondin-1 Repeats Proteinases-5 and -15 Facilitates Myoblast Fusion*

Received for publication, October 20, 2012, and in revised form, December 4, 2012 Published, JBC Papers in Press, December 11, 2012, DOI 10.1074/jbc.M112.429647

**Nicole Stupka[‡1,2], Christopher Kintakas[‡§1,3], Jason D. White[§¶4], Fiona W. Fraser[‡], Michael Hanciu[‡], Noriko Aramaki-Hattori[‖], Sheree Martin[‡], Chantal Coles[§¶], Fiona Collier**, Alister C. Ward[‡], Suneel S. Apte[‖], and Daniel R. McCulloch[‡5]**

*From the [‡]School of Medicine and Molecular and Medical Research SRC, Deakin University, Geelong, Victoria 3216, Australia, the [§]Muscular Dystrophy Research Group, Murdoch Childrens Research Institute, Parkville, Victoria 3052, Australia, the [¶]University of Melbourne Veterinary School, Parkville, Victoria, 3010, Australia, the [‖]Department of Biomedical Engineering, The Cleveland Clinic, Cleveland, Ohio 44195, and **Barwon Health, The Geelong Hospital, Geelong, Victoria 3220, Australia*

**Background:** Skeletal muscle fiber formation requires myoblast cell-cell membrane contact and fusion.
**Results:** A versican-rich pericellular matrix surrounding myoblasts is proteolytically cleared by ADAMTS versicanases facilitating myoblast contact and fusion.
**Conclusion:** Versican processing by ADAMTS versicanases contribute to muscle fiber formation.
**Significance:** Targeting versican remodeling could enhance the regenerative capacity of muscle by improving muscle fiber fusion during regeneration.

**Skeletal muscle development and regeneration requires the fusion of myoblasts into multinucleated myotubes. Because the enzymatic proteolysis of a hyaluronan and versican-rich matrix by ADAMTS versicanases is required for developmental morphogenesis, we hypothesized that the clearance of versican may facilitate the fusion of myoblasts during myogenesis. Here, we used transgenic mice and an *in vitro* model of myoblast fusion, C2C12 cells, to determine a potential role for ADAMTS versicanases. Versican processing was observed during *in vivo* myogenesis at the time when myoblasts were fusing to form multinucleated myotubes. Relevant ADAMTS genes, chief among them *Adamts5* and *Adamts15*, were expressed both in developing embryonic muscle and differentiating C2C12 cells. Reducing the levels of *Adamts5* mRNA *in vitro* impaired myoblast fusion, which could be rescued with catalytically active but not the inactive forms of ADAMTS5 or ADAMTS15. The addition of inactive ADAMTS5, ADAMTS15, or full-length V1 versican effectively impaired myoblast fusion. Finally, the expansion of a hyaluronan and versican-rich matrix was observed upon reducing the levels of *Adamts5* mRNA in myoblasts. These data indicate that these ADAMTS proteinases contribute to the formation of multinucleated myotubes such as is necessary for both skeletal muscle development and during regeneration, by remodeling a versican-rich pericellular matrix of myoblasts. Our study identifies a possible pathway to target for the improvement of myogenesis in a plethora of diseases including cancer cachexia, sarcopenia, and muscular dystrophy.**

The extracellular matrix (ECM)[6] is a functionally critical component of the musculature, because it organizes and assimilates force transmission from contracting muscle fibers to the skeleton. It does so by stabilizing contracting muscle fibers via the membrane dystrophin-glycoprotein complex and by contributing the collagen-rich force transmitting matrix that fuses with tendons (1). Disorders of ECM associated with the dystrophin-glycoprotein complex are among the major causes of myopathies (2). What is not generally appreciated, and remains poorly understood is the potential role of ECM both as a barrier and as a contributor in myogenesis.

Myogenesis is a dynamic process in which proliferating myoblasts align and merge via membrane-membrane fusion to form multinucleated contractile muscle fibers (3, 4). The efficient fusion of myoblasts into muscle fibers and their correct attachment to a highly specialized ECM surrounding those fibers are critical determinants of correct muscle formation, growth, regeneration, and contractile function (1). Thus, myoblast interactions with the ECM and their synthesis of ECM components are important for normal skeletal muscle development and regeneration (5) and as such the ECM needs to be coordinately remodeled during myoblast proliferation and fusion (6). Most embryonic cells and many adult cells have a surrounding matrix named the pericellular matrix, which is rich in hyaluronan (HA) and a HA-bound large proteoglycan, such as aggrecan in cartilage, and versican in most other connective tissue/mes-

* This work was supported, in whole or in part, by National Institutes of Health Grant PO1-HL107147 (to S. A.) and The Financial Markets Foundation for Children Grant 162-2010 (to D. McC., N. S. and A. W.).
[1] Both authors contributed equally.
[2] Supported in part by a National Health and Medical Research Council Peter Doherty Fellowship.
[3] Supported by Postgraduate Scholarships from the Molecular and Medical Research SRC, Deakin University, and Muscular Dystrophy Australia.
[4] Supported in part by Muscular Dystrophy Australia.
[5] To whom correspondence should be addressed: 75 Pigdons Rd., Geelong, Victoria 3216, Australia. Tel.: 61-3-52272838; Fax: 61-3-52272945; E-mail: daniel.mcculloch@deakin.edu.au.

[6] The abbreviations used are: ECM, extracellular matrix; HA, hyaluronan; ADAMTS, a disintegrin-like and metalloproteinase domain with thrombospondin-1 repeats; TIMP-3, tissue inhibitors of metalloproteinase-3.

enchymal cells (7, 8). This aggregating complex binds to cell surface receptors such as CD44, and contributes to formation of a hydrated pericellular matrix with the ability to exclude particulate matter. Functionally, such a matrix can be considered as a transitional matrix, a dynamic entity that is readily remodeled by new matrix synthesis and specific enzymes (9). Such enzymes include hyaluronidases and proteinases capable of clipping the versican core protein. Emerging evidence in the literature suggests that myoblasts may also express a pericellular matrix rich in versican (10, 11). However, the role of versican and its remodeling is poorly defined, even though it may be an important driver in myogenesis and skeletal muscle regeneration.

Four splice variants of versican are known, and are derived from inclusion (or not) of alternative chondroitin sulfate-rich domains named GAG-$\alpha$ or GAG-$\beta$. The isoforms V1 (containing GAG-$\beta$) and V0 (GAG-$\alpha$ or GAG-$\beta$) are the most abundant in non-neural tissues. Several among the 19 ADAMTS (a disintegrin-like and metalloproteinase domain with thrombospondin-1 repeats) proteinases were previously shown to attack the core protein of both versican isoforms at specific cleavage sites. In regard to V1 sequence enumeration, ADAMTS cleavage of the $Glu^{441}$-$Ala^{442}$ peptide bond (12) within the GAG-$\beta$ domain was shown to be crucial in a number of developmental contexts using ADAMTS knock-out mice (13, 14). We hypothesized that during skeletal muscle development, one or more members of the subset of ADAMTS proteinases comprising ADAMTS1, -4, -5, -8, -9, -15, and -20 (13) could be involved in remodeling the versican-rich pericellular matrix to facilitate cell membrane contact and fusion. Therefore, the purpose of this study was to determine the significance of myoblast pericellular matrix and its clearance by ADAMTS proteinases during myotube formation. In particular, we focused on the potential role of ADAMTS5 in remodeling versican, because it is strongly expressed in developing skeletal muscle and cleaves both aggrecan and versican (15–17).

ADAMTS5 is a major target for arthritis therapy because cartilage aggrecan degradation is not seen in mice lacking ADAMTS5 following experimentally induced inflammatory arthritis and osteoarthritis (18, 19). However, ADAMTS5 also has important functions in physiology, particularly during embryonic development. Thus a thorough understanding of its biological function(s) in skeletal muscle is paramount, given arthritis patients are also likely to present with muscle wasting due to the immobilizing nature of the disease. This current study exemplifies the importance of ADAMTS5 and the related versicanase, ADAMTS15, in the process of myoblast fusion leading to mature muscle fiber formation.

## EXPERIMENTAL PROCEDURES

*Mice and Tissues*—Mouse experiments were carried out in accordance with National Health and Medical Research Council guidelines for the care and use of animals in research under the approval of the Animal Welfare Committee, Deakin University. Some experiments were done under an IACUC-approved protocol at the Cleveland Clinic. Six-week-old *C57/Bl6J* (Animal Resources Centre, WA, Australia) mice were mated after 1700 h and conception was confirmed before 0900 h the next morning by observation of vaginal mucous. The morning of conception was designated as gestational age 0.5 days post-coitus (E0.5). Proximal hind limbs of embryonic ages E12.5 through E14.5, or proximal hind limb muscles of older embryos (dissected away from osseous tissue) were collected and stored in TRIzol (Invitrogen, Mulgrave, Australia) at −80 °C for mRNA analyses or fixed in 4% paraformaldehyde for immunostaining. *Adamts5*$^{-/-}$ mice used in this study were from Jackson Laboratories and are as previously described (15, 20).

*Cell Culture*—C2C12 myoblasts were maintained in growth medium (Dulbecco's modified Eagle's medium (DMEM) containing 10% fetal bovine serum (FBS) (Invitrogen)) in an atmosphere of 5% $CO_2$ at 37 °C (HERAcell 150i, Thermo Scientific, Scoresby, Australia). For time course analysis of differentiation, cells were seeded at 20,000 cells/cm$^2$ and collected 24 (proliferation) and 48 h later (when confluent), after which differentiation medium (DMEM + 2% horse serum) was added. For the first 48 h of differentiation, the medium contained 10 $\mu$M Ara-C (Sigma) to stimulate cell cycle withdrawal. The time points were 6 h, 24 h, 48 h, 72 h, 4 days, and 6 days (differentiation). Media was changed every 24 h. Cells were harvested in triplicate wells, collected in TRIzol, and stored at −80 °C. For siRNA transfection, C2C12 myoblasts were seeded into 12-well tissue culture plates at a density of 16,000 cells/cm$^2$ and grown to 60–70% confluence. Cells were transfected with 25 nM Stealth RNAi targeting *Adamts5* (*Adamts5*-1, 5′-gaucuucccgcauccugcaugucuauagacaugcaggaugcgggaagauc-3′; *Adamts5*-2, 5′-caggcuguacagucaugcaagcauuaaugcuugcaugacuguacagccug-3′) or control siRNA oligonucleotides (medium GC content, Invitrogen) diluted in Opti-MEM (Invitrogen) using Lipofectamine RNAi MAX (Invitrogen) according to the manufacturer's instructions. After 5 h, the transfection media were replaced with growth media. Differentiation was induced the following day when the cells reached ~90% confluence by changing to differentiation media. For the first 48 h of differentiation, 10 $\mu$M Ara-C was included to stimulate cell cycle withdrawal. The differentiation medium was changed every 24 h. For the rescue experiments, conditioned medium from HEK293T cells transfected with cDNA expression constructs (see below) was used at a dilution of 1:4 in differentiation media from 24 h differentiation until the experimental end-point (72 h differentiation) when the fusion index was calculated.

*Expression Constructs and Transfection of HEK293T Cells*—HEK293T cells (ATCC, Manassas, VA) were grown in DMEM containing 10% FBS in an atmosphere of 5% $CO_2$ at 37 °C. Cells were transfected using Lipofectamine 2000 (Invitrogen) with constructs encoding *ADAMTS5* (wild type (WT) and $E^{411}A$ (16)), *Adamts15* (WT and $Glu^{343}Ala$), V1 versican construct (kindly provided by Professor Dieter Zimmermann), and empty vector control (pcDNA3.1MycHisA+ (Invitrogen)). Serum-free conditioned medium was collected and cells were harvested in ice-cold PBS with a cell scraper from which cell lysate was prepared as previously described (16, 20–22). Sterile conditioned medium was used for the rescue experiments.

*RNA Extraction, Reverse Transcription, and Quantitative RT-PCR*—RNA was extracted as per the manufacturer's protocol using TRIzol and 1 $\mu$g of total RNA was reverse-transcribed with the iScript cDNA synthesis kit (Bio-Rad). Quantitative

RT-PCR was performed on the cDNA using iQ SYBR Green Supermix (Bio-Rad) and oligonucleotide primers for the genes of interest (20) (additional primer sequences available upon request). Quant-iT OliGreen ssDNA Assay Kit (Invitrogen) was used to quantitate total cDNA input as per the manufacturer's instructions. Relative changes in mRNA levels to proliferating myoblasts were calculated using the $\Delta C_t$ method.

*Western Blotting*—Western blotting under reducing conditions was used to analyze protein expression following the above transfections. Protein samples were electrophoresed on 6 (Versican V1) or 8% (ADAMTS5, ADAMTS15, and G1-DPEAAE) BisTris (2-[bis(2-hydroxyethyl)amino]-2-(hydroxymeth-yl)propane-1,3-diol) acrylamide gels (Bio-Rad) alongside the Precision Plus protein standard (Bio-Rad) and transferred to PVDF membrane (Amersham Biosciences Hybond-P (GE Healthcare, Murarrie, Australia)). Anti-Myc clone 9E10 (Sigma), anti-GAG-$\beta$, anti-DPEAAE, or anti-ADAMTS5 (16, 20, 22, 23) antibodies were used typically between 1/5000 and 1/1000 dilutions. Anti-GAPDH (Millipore) was used to assess levels of protein loading in both cell lysate and conditioned medium (16, 20, 22). Secondary antibodies used were conjugated with horseradish peroxidase (Dako, Australia). Antibody binding was detected on Amersham Biosciences Hyperfilm using ECL or ECL-prime (GE Healthcare).

*Immunocytochemistry and Immunohistochemistry*—C2C12 cells were seeded into LabTek Permanox chamber slides (Electron Microscopy Sciences, Hatfield, PA) in growth medium and differentiated as described above. Cells were fixed in 4% paraformaldehyde/PBS for 5 min at room temperature before proceeding with immunostaining as previously described (20). Immunohistochemistry for V0/V1 versican (GAG-$\beta$), cleaved versican (DPEAAE), and ADAMTS5 was performed as previously described (20), whereas co-localization of desmin included the addition of mouse monoclonal anti-desmin (Abcam, Cambridge, United Kingdom) with either rabbit anti-ADAMTS5 or anti-DPEAAE antibodies. The secondary antibodies used were FITC goat anti-rabbit IgG and Texas Red goat anti-mouse IgG (Invitrogen).

For desmin staining, myotubes were permeabilized using 0.1% Triton X-100 in PBS. Cells were incubated in 1/200 dilution of either rabbit anti-desmin polyclonal primary antibody (Abcam) or mouse monoclonal anti-desmin in PBS containing 1% bovine serum albumin (BSA)/PBS (Sigma). Cells were then incubated with either FITC goat anti-rabbit IgG or Texas Red goat anti-mouse IgG (1:25 dilution) in 1% BSA/PBS. Nuclei were counterstained with either TO-PRO-3 iodide or DAPI (Invitrogen).

*Quantitation of Fusion Index*—For each experimental treatment, 15 digital images were captured with either an IX81 or IX71 Olympus inverted fluorescence microscope and a CC12 or an XM10 camera (Olympus). A well formed myotube was identified and an image of the founder myotube was captured, followed by two random images in the immediate vicinity (within 2 fields of view). This process was repeated for a total of five times, yielding 15 images per experimental group per experiment. To determine the fusion index, nuclei were counted and designated as either fused or unfused, using the Count tool in Adobe Photoshop CS5 Extended (Version 12.0) software. Fusion index was calculated as the percentage of fused nuclei as a proportion of total nuclei. Myoblasts were considered to be unfused if the cell contained only one or two nuclei; myotubes with three nuclei per cell were considered to be nascent myotubes for the purpose of calculating fusion index. Three independent experiments, performed in duplicate, were used for the determination of fusion index and ~2,000–2500 nuclei were counted per experimental condition, per experiment.

To assess the effect of *Adamt5* siRNA treatment on nascent myotube formation and maturation, the total number of myotubes per field of view was counted whereby myotubes containing 2–4 nuclei were designated as nascent and 5–9 nuclei or 10+ nuclei were designated as mature (24–26). Approximately 520–570 myotubes were counted per control or siRNA-treated groups across 6 independent experiments each performed in duplicate.

*Creatine Kinase Activity Assay and Measurement of Total TGF-$\beta$*—Cells were lysed with 150 $\mu$l of lysis buffer containing 40 mM MES buffer, 50 mM Trizma (Tris base), 1% Triton X-100, 1× protease inhibitor mixture (Roche Applied Science). Insoluble material was collected by centrifugation and the supernatant was used for analysis of creatine kinase activity. Three technical replicates for each sample were performed in a 96-well plate using creatine kinase-NAC (Thermo Scientific). Creatine kinase activity was measured by the change in absorbance at 340 nm over 3 min (20-s intervals) at 37 °C. Units per liter (units/liter) was calculated using the following formula: $Ik = (TV \times 1000)/(A \times \mathrm{SV} \times P)$, where $TV$ is the total reaction volume (0.210 ml), $A$ is the millimolar absorption coefficient of NADH at 340 nM (6.3), $SV$ is the sample volume (0.010 ml), and $P$ is the unique path length of light in the 96-well plate (determined to be 0.533 cm by spectrophotometric comparison of absorbance with known path lengths). Total levels of TGF-$\beta$ were measured in 40-$\mu$l aliquots of media collected from C2C12 cell cultures by an ELISA (R&D Systems, Minneapolis, MN) as per the manufacturer's instructions.

*Cell Viability Counts*—After 24 h differentiation, dead cells were collected and adherent cells were trypsinized and collected into the same FACS tube. The cells were resuspended in 100 $\mu$l of 0.2% BSA/PBS containing 7-aminoactinomycin D. Cells were washed in PBS and fixed in 1% formaldehyde containing 2% FBS and 2 $\mu$g/ml of actinomycin. The percentage of viable cells was determined by flow cytometric analysis using CELLQuest software. Cell number and viability was also determined using trypan blue (Sigma) exclusion staining and manual cell counts on a hemocytometer.

*Particle Exclusion Assay and Quantitation of Pericellular Matrix Area*—The assay was done essentially as previously described by Hattori *et al.* (27). C2C12 myoblasts transfected with *Adamts5* siRNA were trypsinized and re-plated at a density of ~2,000 cells/well into 6-well plates 24 h after siRNA transfection. Cells were cultured for another 24 h and stained with 1 $\mu$M calcein AM (Sigma). The medium was changed after 30 min and a red blood cell (RBC) suspension in serum-free DMEM at a density of $1 \times 10^8$ erythrocytes/ml was added. After RBCs had settled to the bottom, images were taken with an Olympus IX71 inverted microscope (FITC channel for calcein-

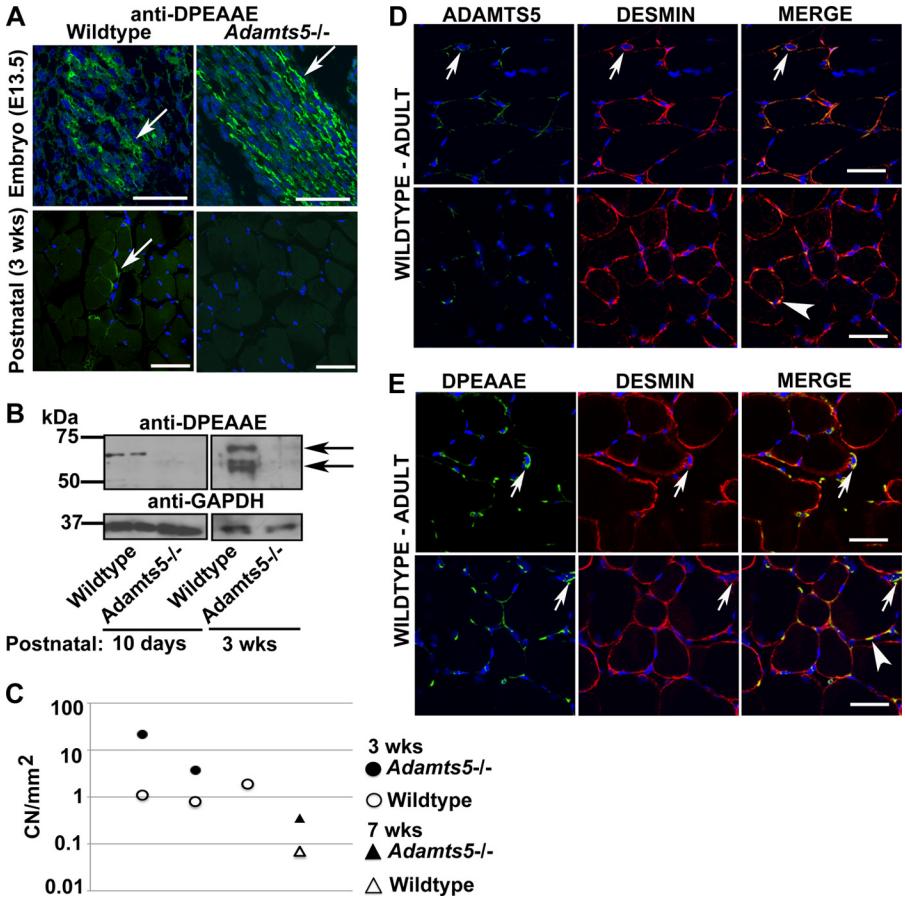


FIGURE 1. **Versican is proteolytically cleaved in embryonic and juvenile skeletal muscle.** *A,* versican cleavage using anti-DPEAAE immunofluorescence (*green* signal, nuclei stained *blue* with DAPI) is readily detectable (*arrows*) in developing skeletal muscle of wild type and *Adamts5*$^{-/-}$ mice at embryonic age (E) 13.5 days (*top panels*). It remains visible in 3-week-old wild type mice but not *Adamts5*$^{-/-}$ mice (*lower panels*). *Scale bars* = 100 $\mu$m. The data are representative of embryonic hind limbs and 3-week-old skeletal muscle from 3 separate mice for each genotype. *B,* Western blot using anti-DPEAAE showing that versican cleavage at position E$^{441}$A (V1) is detectable in postnatal skeletal muscle (*black arrows*) of wild type mice but absent in *Adamts5*$^{-/-}$ mice. The Western blot shows two 10-day-old wild type and *Adamts5*$^{-/-}$ mice skeletal hind limb muscle lysates, respectively (*left-hand panel*), and one 3-week-old wild type and *Adamts5*$^{-/-}$ mice skeletal hind limb muscle lysates, respectively (*right-hand panel*). *C, Adamts5*$^{-/-}$ mice have a greater number of centrally located nuclei than wild type mice in postnatal skeletal muscle (3 and 7 weeks old). *D,* ADAMTS5 co-localized with desmin in mature skeletal muscle fibers (*arrowhead*) and satellite cells (*arrows*). *Scale bars* = 50 $\mu$m. *E,* versican cleavage (DPEAAE neo-epitope) co-localized with desmin in mature skeletal muscle fibers (*arrowhead*) and satellite cells (*arrows*). *Scale bars* = 50 $\mu$m. The data for *D* and *E* represent muscle sections from 2 independent mice and these observations are representative of wild type mice ($n$ = 4).

labeled cells and bright field for RBCs). As a control, hyaluronidase digestion was done using *Streptomyces hyalurolyticus* hyaluronidase (Sigma) prior to the particle exclusion assay. Resultant images of controls or *Adamts5*-1 siRNA treatments were analyzed using custom, semiautomated scripts generated in Image-Pro version 6.2 (Media Cybernetics, Silver Springs, MD) as previously described (27). In addition, scoring of the RBC exclusion area was performed by 3 investigators blinded to the experimental groups using a scale of 0–3, where 0 = no matrix accumulation and 3 = maximal matrix accumulation. Approximately 20 images per experimental group were randomized and coded before the investigators scored them. Scores were whole number values only from 0 to 3, *i.e.* either 0, 1, 2, or 3.

*Statistics*—For quantitative PCR analyses, one-way analysis of variance followed by a Tukey's post hoc analysis were performed. All other analyses were performed using a Student paired, two-tailed $t$ test between control and test groups. Gaussian distribution was assumed in all cases. Data were considered statistically significant when a $p$ value $< 0.05$ was obtained.

## RESULTS

*Versican Processing Is Absent in Postnatal Skeletal Muscle of Adamts5*$^{-/-}$ *Mice*—ADAMTS5 shows strong versicanase activity compared with other proteoglycan-degrading ADAMTS members (14); however, *Adamts5*$^{-/-}$ mice do not display an overt myopathy (15, 19). In both wild type and *Adamts5*$^{-/-}$ embryonic hindlimb muscles versican processing was readily detectable by immunostaining with the neo-epitope antibody anti-DPEAAE that specifically detects the ADAMTS cleavage site in the V0 and V1 splice variants of versican (16, 20, 28, 29) (Fig. 1*A, top panels*). These data suggest that versican processing is unimpaired in *Adamts5*$^{-/-}$ mice during myogenesis, potentially as a result of participation by other proteinases. In contrast to wild type muscle, juvenile and mature skeletal muscle from 10 to 13 days and 3 weeks postnatal *Adamts5*$^{-/-}$ mice had barely detectable versican cleavage when analyzed by

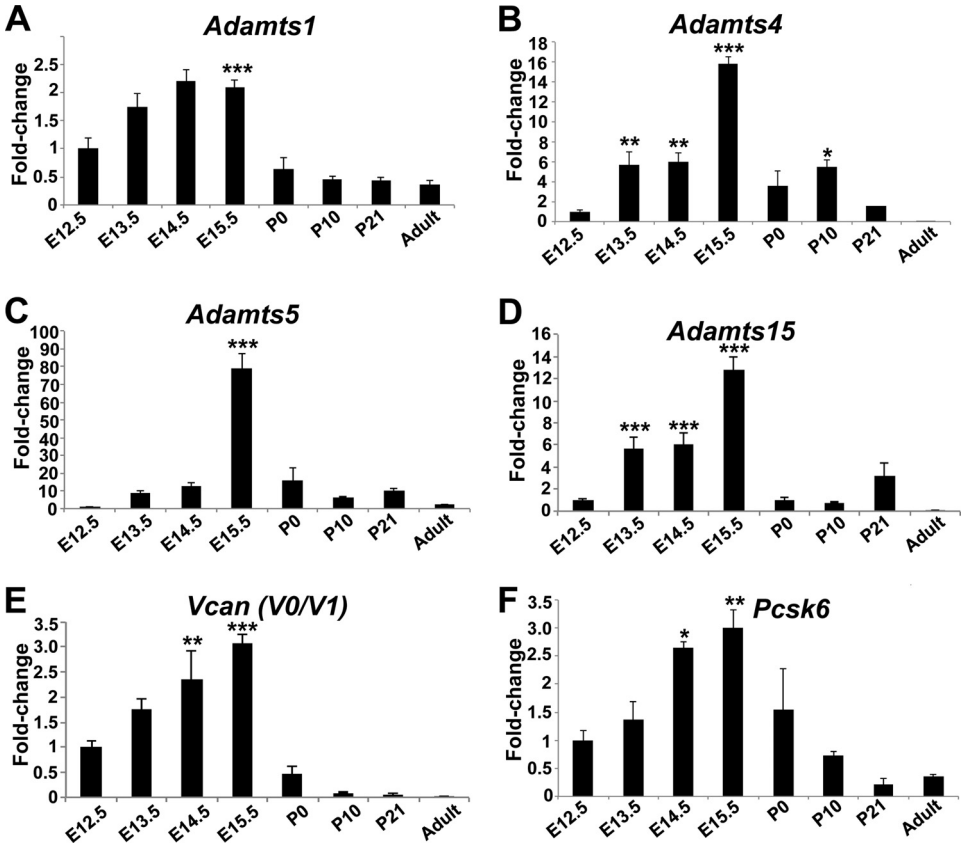


FIGURE 2. **Quantitative RT-PCR of *Adamts1, -4, -5,* and *-15* mRNA (*A-D*, respectively), *Vcan* mRNA (V0/V1) (*E*), and *Pcsk6* mRNA (*F*) in developing hind limb skeletal muscle.** All genes were significantly up-regulated during embryonic myogenesis with a concordant decrease in postnatal expression. $N = 3$ hind limbs per embryonic (*E*) or postnatal (*P*) stage. The data are presented as fold-changes in levels of mRNA relative to E12.5 hind limbs. Adult = 6–8 weeks old. *, $p < 0.05$; **, $p < 0.01$; ***, $p < 0.001$. *Error bars* represent S.E.

immunohistochemistry (Fig. 1*A*, *bottom panels*) or immunoblotting (Fig. 1*B*). This suggests that ADAMTS5 has a substantial role in versican processing in postnatal skeletal muscle growth and maturation. In agreement with this, higher levels of centrally positioned nuclei were seen in 3- and 7-week-old *Adamts5*$^{-/-}$ mice compared with wild type mice (Fig. 1*C*). The presence of central nuclei suggests the absence of ADAMTS5 delayed maturation during postnatal muscle growth (30). Adult wild type skeletal muscle showed co-localization of ADAMTS5 (Fig. 1*D*) and cleaved versican (Fig. 1*E*) with desmin around mature muscle fibers and satellite cells, thus associating versican processing with functional skeletal muscle.

*ADAMTS Proteases Are Dynamically Expressed throughout Embryonic Skeletal Muscle Development and during in Vitro Myotube Formation*—We previously demonstrated prominent expression of *Adamts5* mRNA in developing mouse skeletal muscle (15). Quantitative RT-PCR for *Adamts* genes of interest in embryonic skeletal muscle demonstrated significantly increased *Adamts1*, *Adamts4*, *Adamts5*, and *Adamts15* mRNA between embryonic ages 13.5 and 15.5 days post-coitus (E13.5–E15.5), with maximal expression observed at E15.5, coincident with myoblast fusion (Fig. 2, *A-D*). mRNA for *Vcan* V0/V1 splice variants also increased concurrently (Fig. 2*E*), along with *Pcsk6*, which encodes PACE4, a proprotein convertase known to activate ADAMTS5 extracellularly (17) (Fig. 2*F*). Myogenin, a muscle regulatory factor and marker of myotube fusion, was also significantly up-regulated compared with adult skeletal muscle as expected (Fig. 4*A*).

To elucidate the function for the ADAMTS proteolysis of versican during skeletal muscle development, we used a well characterized *in vitro* cell model of myoblast fusion, the C2C12 cell line (31). These cells remain undifferentiated in rich serum, but spontaneously undergo differentiation along a well characterized pathway when grown in a nutritionally poor medium containing horse serum. Quantitative RT-PCR showed that *Adamts1, Adamts4, Adamts5,* and *Adamts15* mRNAs were dynamically up-regulated soon after induction of myoblast differentiation (Fig. 3, *A-D*), whereas *Vcan* mRNA was dramatically up-regulated upon myoblasts reaching confluence and contact inhibition, remaining high throughout the differentiation process (Fig. 3*E*). *Pcsk6* mRNA was also dramatically up-regulated at 72 h after onset of differentiation when myotube fusion is occurring (Fig. 3*F*). Maximal levels of myogenin up-regulation were observed at 24 h with commencement of myotube formation (Fig. 4*A′*). RT-PCR showed that the versican V1 isoform was the major splice variant expressed both in E13.5 skeletal muscle and C2C12 myoblasts (Fig. 4*B*).

Next, we evaluated C2C12 cell expression of versican, cleaved versican, and ADAMTS5 during differentiation by confocal microscopy, using anti-versican GAG-$\beta$, anti-DPEAAE, and anti-ADAMTS5 antibodies (20). Pericellular versican accumulation was detected as early as 6 h after onset of differ-

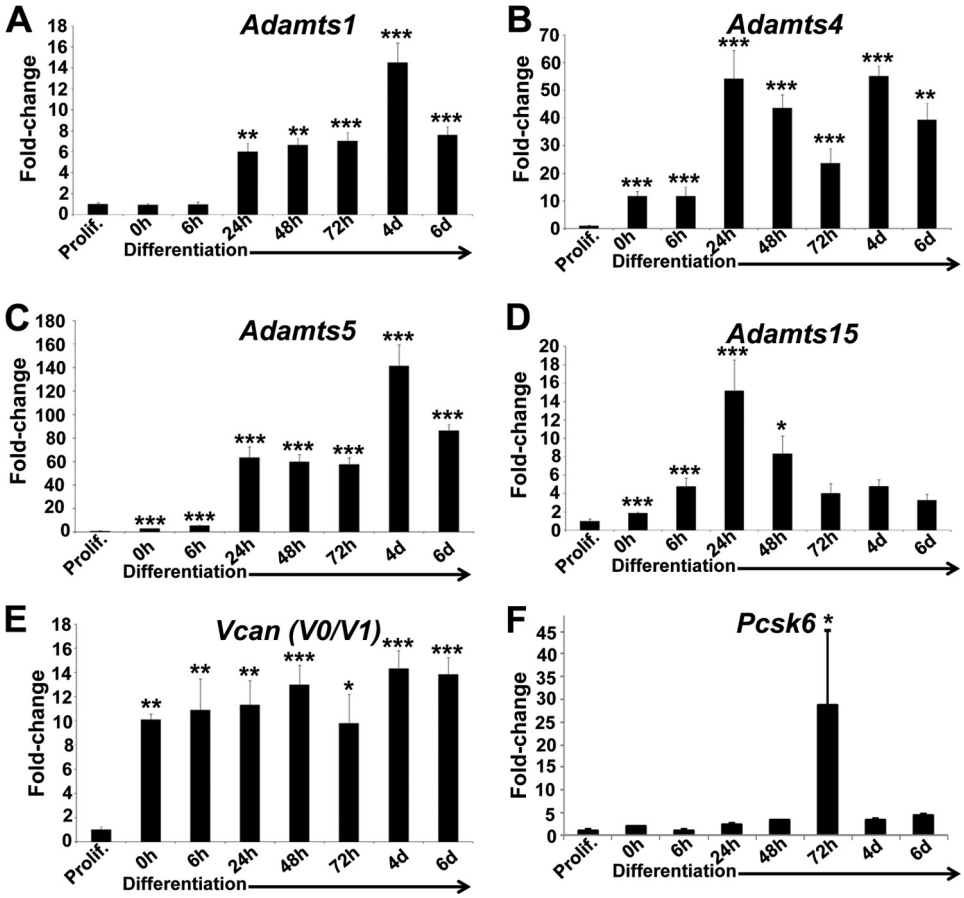


FIGURE 3. **Quantitative RT-PCR of *Adamts1, -4, -5,* and *-15* mRNA (*A–D*, respectively), *Vcan* mRNA (V0/V1) (*E*), and *Pcsk6* mRNA (*F*) during differentiation of C2C12 myoblasts *in vitro*.** All genes were significantly up-regulated during myoblast differentiation relative to proliferating, subconfluent cells with a concordant decrease in expression after onset of differentiation, except for *Vcan*, whose mRNA levels rose once cells reached confluence and remained high (*E*). The data are presented as fold-changes in levels of mRNA relative to proliferating myoblasts (*Prolif.*). 3 Biological replicates of each time point were performed in duplicate (*h* = hours, *d* = days). *, $p < 0.05$; **, $p < 0.01$; ***, $p < 0.001$. *Error bars* represent S.E.

entiation when the myoblasts appeared nestled within a versican-rich matrix alongside detectable versican cleavage (Fig. 4*C, top panels*). After 72 h differentiation, both ADAMTS5 and DPEAAE were localized at the ends of fusing myoblasts (Fig. 4*C, bottom panels*), suggesting a role for versican clearance, which could facilitate cell-cell contact and membrane fusion during myotube formation.

*Catalytically Active ADAMTS5 and ADAMTS15 Proteinases Facilitate Myoblast Fusion*—Given these parallels between the gene expression profiles and versican processing in embryonic muscle and *in vitro* myogenesis, we investigated the role of ADAMTS5 in the C2C12 cell line model. *Adamts5* was targeted using two independent siRNA sequences each of which resulted in a 60–75% reduction in *Adamts5* mRNA levels (Fig. 5*A*) with a modest decrease in intracellular ADAMTS5 (Fig. 5*B*). Upon silencing *Adamts5* mRNA, myogenin expression was reduced (Fig. 5*C*) and the myotubes formed were smaller and contained fewer nuclei (Fig. 5*D*) with a significant reduction in the fusion index (Fig. 5*E*), and creatine kinase activity (Fig. 5*F*). Of the two siRNA used, *Adamts5*-1 siRNA, showed the stronger reduction in *Adamts5* mRNA levels. In separate experiments, manual cell counts and 7-aminoactinomycin D staining showed *Adamts5* siRNA treatment did not reduce cell viability (data not shown). Further assessment of myotube formation and maturity showed significantly less mature myotubes (5+ nuclei (24–26)) formed following *Adamts5* siRNA treatment (Fig. 5*G*) alongside less total myotubes formed, suggestive of an initial impairment of myoblast fusion into nascent myotubes (Fig. 5*G*).

To validate the observed effects as being a consequence of specific siRNA targeting of *Adamts5*, and to determine whether ADAMTS proteolytic activity could indeed facilitate myotube fusion, we attempted to reverse the effects of siRNA using serum-free conditioned media containing either catalytically active or inactive ($E^{411}A$ active site mutant) human ADAMTS5 (16) or either catalytically active or inactive ($Glu^{343}Ala$ active-site mutant) mouse ADAMTS15 (data not shown).[7] Fraser, F. W., Dancevic, C. M., Stupka, N., Ward, A. C., and McCulloch, D. R. The Expression and Biosynthesis of A Disintegrin-like and Metalloproteinase Domain with Thrombospondin Repeats -15; A Novel Versican Cleaving Proteoglycanase. Submitted to: the Journal of Biological Chemistry (currently under revision). These were added to the C2C12 differentiation medium 24 h after siRNA transfection until the differentiation end point. The catalytically active forms, but not the inactive mutants of

[7] Fiona W. Fraser, Carolyn M. Dancevic, Nicole Stupka, Alister C. Ward, and Daniel R. McCulloch, submitted for publication.

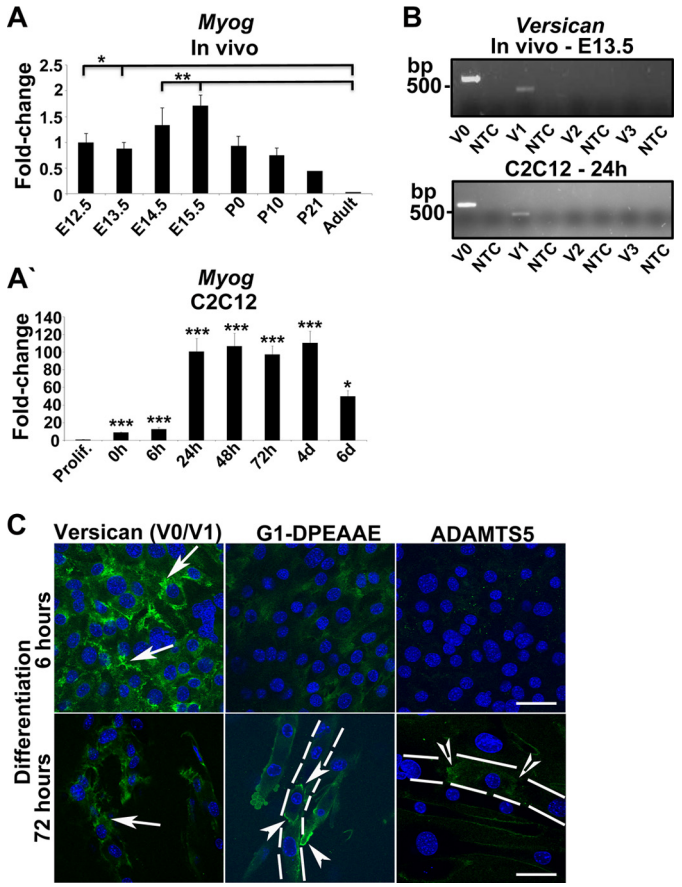


FIGURE 4. **Association of myogenin mRNA and versican splice variants in embryonic skeletal muscle and C2C12 myoblasts, immunodetection of versican, cleaved versican, and ADAMTS5 in myoblast differentiation.** *A,* significantly higher levels of myogenin mRNA is present in developing skeletal muscle extracted from mouse embryonic limbs compared with adult skeletal muscle. 3 Limbs per embryonic (*E*) or postnatal (*P*) stage were used. Adult = 6–8 weeks old. *A′*, myogenin mRNA expression increases significantly throughout C2C12 myoblast differentiation (*h* = hours, *d* = days). *B,* versican V0 and V1 splice variants are the predominant versican mRNA species expressed in developing skeletal muscle (*top panel*) and C2C12 myoblasts (*bottom panel*). NTC = no template control. *C*, the panels show immunofluorescent detection of the versican GAG-$\beta$ domain, cleaved versican (G1-DPEAAE), and ADAMTS5 (green, nuclei stained blue with DAPI) in early differentiated myoblasts (6 h) and late (72 h) differentiated myotubes by immunocytochemistry. Staining with the antibody raised to the GAG-$\beta$ domain of versican (V0/V1) is indicated by *arrows*, G1-DPEAAE immunostaining with *arrowheads*, and ADAMTS5 with *open arrowheads*. *White dashed lines* outline myotubes. Note the pattern of versican cleavage at the ends of fusing myoblasts (*arrowheads*). The data are representative of 3 biological replicates of each time point performed in duplicate ($n = 3$) . *Scale bars* = 50 $\mu$m. For *A* and *A′*, *, $p < 0.05$; **, $p < 0.01$; ***, $p < 0.001$, *error bars* = S.E.

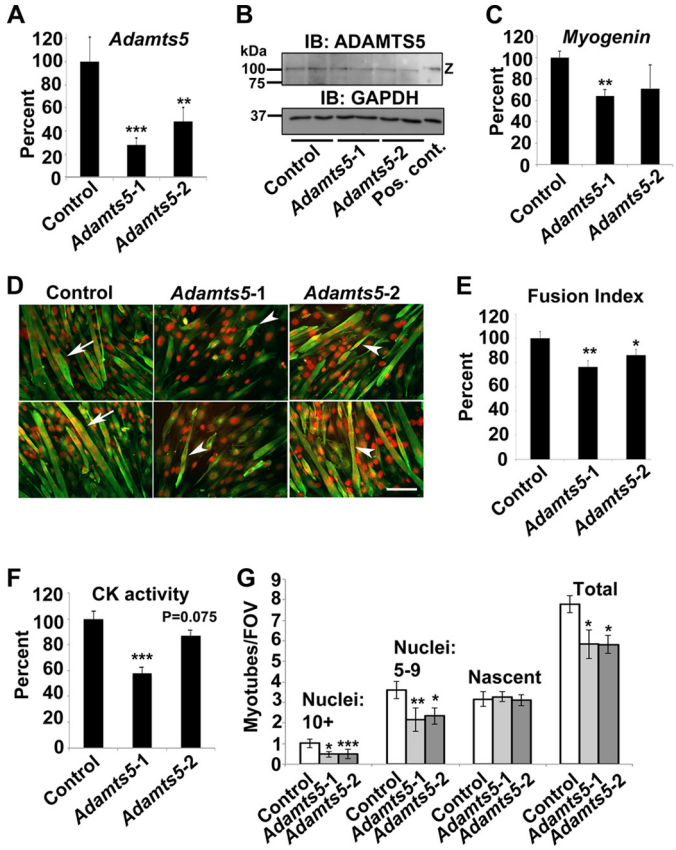


FIGURE 5. **Adamts5 siRNA reduces myoblast fusion and myotube maturation.** *A,* significant knockdown of *Adamts5* mRNA levels upon siRNA treatments are seen at 72 h after differentiation. siRNA *Adamts5*-1 led to greater mRNA silencing. *B,* a modest decrease in intracellular ADAMTS5 protein levels is observed upon siRNA treatments. *Pos. Cont.* = positive control (ADAMTS5 transfected HEK293T cells, which migrates at a higher apparent molecular weight due to the presence of a Myc-$His_6$ tag). *C,* reduced myogenin mRNA is observed in the *Adamts5* siRNA-treated groups indicative of reduced differentiation. *D,* representative images of C2C12 myotubes at 72 h differentiation stained with desmin (*green*) and TO-PRO®-3 (*red*). Control (scrambled G-C matched siRNA) treated myotubes shows efficient fusion (*arrows*). Two siRNAs targeted to separate regions of *Adamts5* mRNA (*Adamts5*-1 or *Adamts5*-2) reduce myotube fusion and the myotubes formed in those siRNA groups are shorter and narrower (*arrowheads*). *Scale bar* = 100 $\mu$m. *E,* the calculated fusion index of $n = 3$ biological replicates performed in duplicate, whose images are represented in *A*. Significantly less fusion is observed in the *Adamts5* siRNA-treated groups. *F,* significantly less creatine kinase (*CK*) is present in the medium of the *Adamts5* siRNA-treated groups. *G*, significantly fewer mature myotubes (5+ nuclei) and total myotubes are formed upon siRNA treatments. The data are representative of 6 biological replicates performed in duplicate. In all cases: *, $p < 0.05$; **, $p < 0.01$; ***, $p < 0.001$; *error bars* = S.E.

both these ADAMTS versicanases effectively restored the fusion defect back to control levels (Fig. 6, *A* and *B*), indicating that ADAMTS versicanase catalytic activity is required for myotube fusion and suggesting that ADAMTS15, was as effective as ADAMTS5. Indeed, ADAMTS15 is now known to be a versican-degrading proteinase[7] and may compensate where ADAMTS5 activity is reduced. When we added ADAMTS5 and ADAMTS15 conditioned medium to differentiating myoblasts without prior *Adamts5* siRNA treatment, we observed that neither catalytically active proteinase enhanced myotube fusion above the control (data not shown). In contrast, both catalytically inactive ADAMTS5 and ADAMTS15 impaired fusion by ~20 ($p < 0.05$) and ~30% ($p < 0.01$), respectively, suggestive of a dominant-negative effect, such as could occur by binding to versican or other substrates involved in myogenesis and preventing cleavage by ambient ADAMTS proteinases. In separate experiments, full-length V1 versican containing conditioned medium from HEK293T cells was added to the C2C12 media, leading to a ~70% reduction in fusion compared with empty vector control conditioned medium ($p < 0.001$, data not shown).

*Reduced Adamts5 mRNA Results in the Accumulation of Pericellular Matrix Around C2C12 Myoblasts*—Using the red blood cell exclusion assay (27), a significant increase in pericellular matrix was observed after treatment with *Adamts5* targeted siRNA, using either computer imaging (Fig. 7, *A* and *B*, *Adamts5*-1 siRNA *versus* control) or blinded visual analysis,

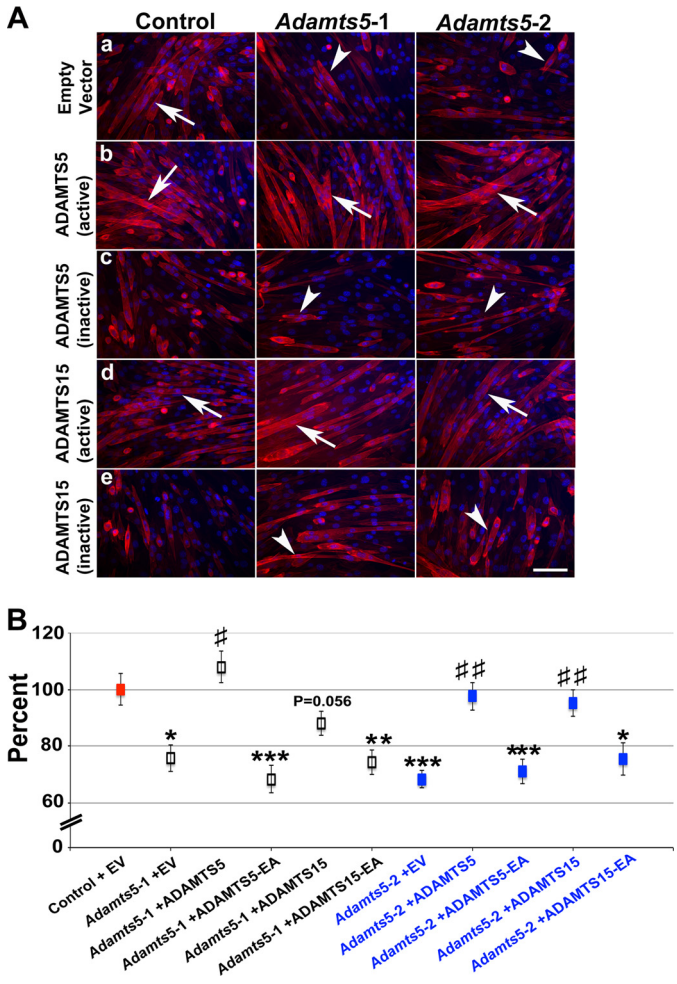


FIGURE 6. **Addition of active ADAMTS5 or ADAMTS15 rescues the fusion defect resulting from *Adamts5* siRNA treatment.** *A,* representative images of C2C12 myotubes at 72 h differentiation stained with desmin (*red*) and nuclear DAPI (*blue*). *a*, control (scrambled G-C matched siRNA) or *Adamts5* siRNA (*Adamts5*-1 or *Adamts5*-2)-treated myotubes were incubated in conditioned medium from cells transfected with empty vector (EV in *panel B*) or vectors expressing active and inactive forms of ADAMTS5 and ADAMTS15 as indicated. *b,* the addition of conditioned medium containing active ADAMTS5 rescues the fusion defect caused by *Adamts5* siRNA treatment (*arrows*). *c,* the addition of conditioned medium containing inactive ADAMTS5 ($E^{411}A$) does not rescue the fusion defect caused by *Adamts5* siRNA treatment (*arrowheads*). *d,* the addition of conditioned medium containing active ADAMTS15 rescues the fusion defect caused by *Adamts5* siRNA treatment (*arrows*). *e,* the addition of conditioned medium containing inactive ADAMTS15 ($E^{343}A$) does not rescue the fusion defect caused by *Adamts5* siRNA treatment (*arrowheads*). *Scale bar* = 100 $\mu$m. *B,* the calculated fusion index of 3 biological replicates performed in duplicate whose images are represented in *A*. *, $p < 0.01$; **, $p < 0.001$; ***, $p < 0.0001$ *versus* Control + EV (*red box*); #, $p < 0.0001$ *versus Adamts5*-1 (siRNA) + EV; ##, $p < 0.0001$ *versus Adamts5*-2 (siRNA) + EV. *Error bars* = S.E.

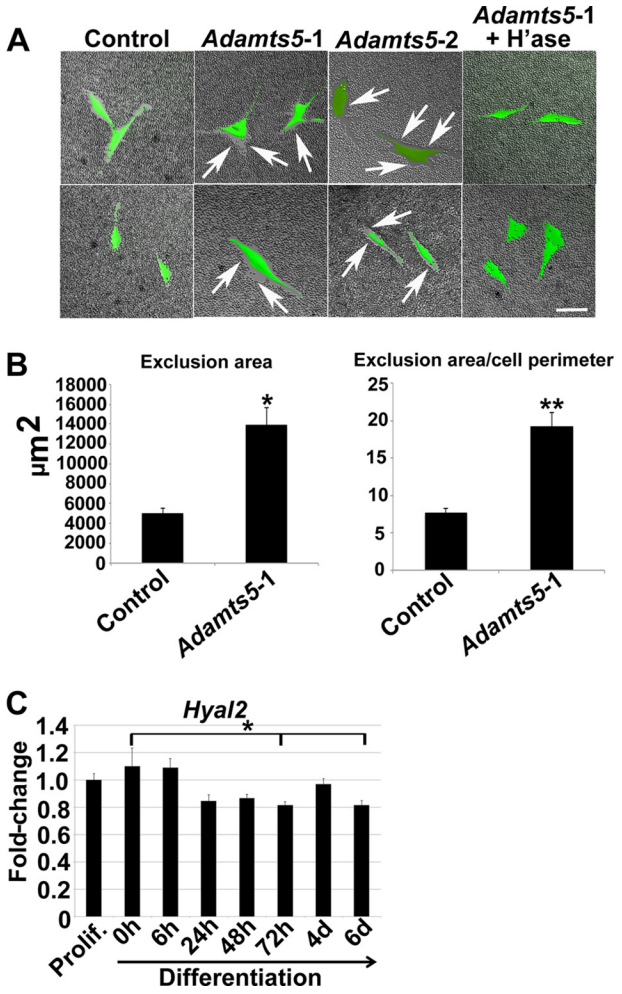


FIGURE 7. **Treatment of C2C12 myoblasts with *Adamts5* siRNA results in accumulation of pericellular matrix, quantitative RT-PCR levels of *Hyal2*.** *A,* two siRNAs targeted to separate regions of *Adamts5* mRNA (*Adamts5*-1 or *Adamts5*-2) cause an accumulation of pericellular matrix in C2C12 myoblasts as shown by the exclusion of red blood cells (*arrows*). *Control* = scrambled G-C matched siRNA. H'ase = hyaluronidase. *Scale bar* = 100 $\mu$m. *B,* quantitation of the area of pericellular matrix exclusion represented in *A* (control ($n = 23$) *versus Adamts5*-1 ($n = 24$) images taken randomly from 3 biological replicate experiments performed in duplicate). *, $p < 0.0001$; **, $p < 0.000001$. *C, Hyal2* mRNA levels are modestly decreased at 72 h and 6 days differentiation in C2C12 cells. The data are presented as fold-changes in levels of mRNA relative to proliferating myoblasts (*Prolif.*). 3 biological replicates of each time point were performed in duplicate (*h* = hours, *d* = days). *, $p < 0.05$. *Error bars* represent S.E.

which included both *Adamts5*-1 and *Adamts5*-2 siRNA groups (data not shown). To ensure the pericellular matrix visualized was hyaluronan-based (and thus versican containing), *Streptomyces* hyaluronidase was added to siRNA-treated C2C12 myoblasts, which eliminated red blood cell exclusion (Fig. 7*A*, *far right panel*).

Because it is likely that hyaluronidase activity is also implicated in the clearance of the hyaluronan and versican-rich pericellular matrix surrounding myoblasts, we analyzed the expression of *Hyal2* across C2C12 differentiation but only modest changes in mRNA expression were observed (Fig. 7*C*). Thus, we conclude that the clearance of a versican-rich pericellular matrix by ADAMTS versicanases contribute to remodeling the pericellular matrix to enable myoblast fusion (Fig. 8).

## DISCUSSION

The presence of a hyaluronate-rich pericellular matrix surrounding myoblasts derived from skeletal muscle was first described by Orkin *et al.* (32). In cardiac muscle, the disappearance of a hyaluronan-rich pericellular matrix coincided with myoblast fusion and altered levels of hyaluronan were also documented during myogenesis by Raganathan and Datta (33). Changes in pericellular matrix chondroitin sulfate proteoglycans during myogenesis were subsequently noted by Carrino *et al.* (34) in developing skeletal muscles of chick embryos; however, the mechanisms and functional consequence of pericellu-

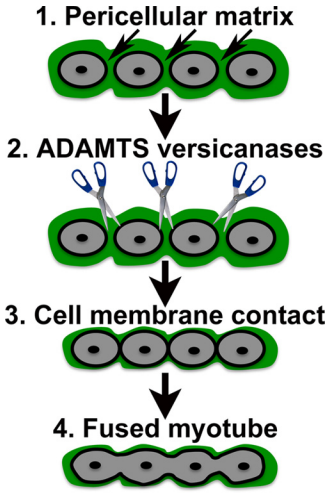


FIGURE 8. **Hypothetical model of myoblast fusion facilitated by pericellular matrix removal.** *1,* myoblasts align nestled within a versican-rich pericellular matrix. *2,* ADAMTS proteases clear the pericellular matrix (*scissors*) surrounding the myoblasts. *3,* myoblasts are denuded of their pericellular matrix especially at approximating ends, allowing cell membrane contact. *4,* myoblasts fuse to form multinucleated myotubes.

lar matrix remodeling in myoblasts and during myoblast fusion has thus far been poorly characterized. We previously noted the expression of *Adamts5* and its co-localization with myosin heavy chain in embryonic mouse hind limbs at a time when myoblasts initiate fusion into multinucleated tubes (15), which was supported by another study (35). ADAMTS versicanases including ADAMTS5 are localized to the cell surface or within the pericellular matrix of cell types such as chondrocytes (36, 37) and it was therefore reasonable to hypothesize they might direct their activity toward versican in myoblasts.

The dynamic regulation of *Adamts* versicanases during *in vivo* and *in vitro* myotube formation suggested synergistic roles in processing of versican and other potential substrates during this process. The presence of ADAMTS5 in the pericellular matrix of C2C12 myoblasts, and its co-localization with cleaved versican (DPEAAE neoepitope) suggested that versican processing by this proteinase could facilitate myoblast fusion. Versican expression was recently shown to regulate proliferation and differentiation of avian myoblasts *in vitro* (38), whereas our data shows the specific relevance of versican proteolysis by ADAMTS versicanases during myoblast fusion to form nascent myotubes and a further requirement in facilitating the process of myotube maturation.

Recent studies identified a role for pericellular matrix clearance in isolated dermal fibroblasts from *Adamts5*$^{-/-}$ mice (27, 39) concomitant with increased or altered TGF-$\beta$ signaling. In partial agreement with those data, we found the pericellular matrix was expanded upon silencing *Adamts5* in the *in vitro* cell model of myogenesis; however, total TGF-$\beta$ levels were unaffected by reducing *Adamts5* levels in this process (data not shown). This observation allowed us to conclude that the accumulation of extracellular matrix was not a direct effect of changes in TGF-$\beta$ levels, but rather is due to reduced processing by ADAMTS versicanases.

An endogenous inhibitor of ADAMTS5 and the related versicanase ADAMTS4 is TIMP-3 (40), which was previously reported as a regulator of myogenesis in C2C12 cells (41); although the overexpression of TIMP-3 inhibited myotube formation, a concordant reduction in TNF-$\alpha$ levels were observed suggesting an ADAM17-mediated effect. Furthermore, the overexpression of TIMP-3 alongside the addition of recombinant TNF-$\alpha$ effectively restored myotube formation (41). Thus, although TIMP-3 clearly has the capacity to inhibit several MMPs, ADAMs, and ADAMTS, some of which are important versicanases, the main action of TIMP-3 is to inhibit ADAM17 processing of TNF-$\alpha$ during myogenesis.

The *Adamts5*$^{-/-}$ mouse presents with no overt myopathy or deficit in gait and mobility, likely due to compensation by other ADAMTS proteinases processing versican, although we did observe higher levels of centrally positioned nuclei in myofibers during postnatal growth. Initial postnatal muscle growth up to ~3 weeks of age is believed to be dependent upon satellite cell activation to form myoblasts, and their proliferation and fusion with existing myofibers, as there is little change in total myofiber number (42). Interestingly, we also showed that ADAMTS5 and cleaved versican localized to mature functional skeletal muscle fibers and satellite cells, indicating a possible role for ADAMTS versicanases during skeletal muscle homeostasis and, potentially, satellite cell activation and skeletal muscle growth.

The proteolysis of versican by ADAMTS proteinases is implicated in morphogenesis of the myocardium, heart valves, secondary palate, urogenital system (43–45), and interdigital web regression (20) during mouse embryogenesis, as well as ovulation in female mice (28, 46). ADAMTS proteinases act alone or cooperatively in some of these contexts, such as web regression and palate closure. Despite combinatorial deletion of five alleles of three *Adamts* genes in mice (*Adamst5*, *Adamts20*, and *Adamts9),* skeletal muscle dysfunction was not elucidated (20). *Adamts4* and *Adamts5* combinatorial knockout mice have been previously reported as having no overt skeletal muscle myopathy (20, 47) further suggesting a compensating role for *Adamts15* during skeletal muscle development.

Skeletal muscle regeneration occurs after mechanical stress such as intense physical activity or trauma. In healthy skeletal muscle the regenerative process is usually relatively efficient. However, aging or muscle dystrophy can increase susceptibility to damage and impair regeneration. In a key feature of the regenerative process, myogenin-expressing myoblasts exit the cell cycle, align with other myoblasts, and fuse to form multinucleated myotubes, which ultimately fuse to existing muscle fibers (48). The current work demonstrated that suppressing ADAMTS5 or ADAMTS15 expression in myoblasts *in vitro* resulted in the impairment of myoblast fusion and subsequent myotube formation. Thus, inhibiting ADAMTS5 in the case of treatment for arthritis could be potentially detrimental in patients with compromised skeletal muscle. In addition, our data showed that catalytically inactive ADAMTS5, which nevertheless, retains substrate-binding ability impaired myoblast fusion. In agreement with this, addition of full-length V1 versican inhibited myoblast fusion, and pericellular matrix expanded upon silencing *Adamts5*.

Collectively, these data strongly suggest that ADAMTS versicanase activity mediates clearance of the pericellular matrix,

which facilitates myotube formation, and that excess versican can impair this process. Our data support the notion that remodeling the transitional matrix is important for proper myotube formation. Thus, this work identifies a novel functional context for ADAMTS proteolytic activity during skeletal muscle development, and potentially, regeneration.

*Acknowledgment—We thank Dr. Liam Hunt for help with blind scoring of the red blood cell particle exclusion assay.*

## REFERENCES


1. Grounds, M. D., Sorokin, L., and White, J. (2005) Strength at the extracellular matrix-muscle interface. *Scand. J. Med. Sci. Sports* **15,** 381–391
2. Reed, U. C. (2009) Congenital muscular dystrophy. Part I. A review of phenotypical and diagnostic aspects. *Arq. Neuropsiquiatr.* **67,** 144–168
3. Horsley, V., and Pavlath, G. K. (2004) Forming a multinucleated cell. Molecules that regulate myoblast fusion. *Cells Tissues Organs* **176,** 67–78
4. Abmayr, S. M., and Pavlath, G. K. (2012) Myoblast fusion. Lessons from flies and mice. *Development* **139,** 641–656
5. Melo, F., Carey, D. J., and Brandan, E. (1996) Extracellular matrix is required for skeletal muscle differentiation but not myogenin expression. *J. Cell Biochem.* **62,** 227–239
6. Calve, S., and Simon, H. G. (2012) Biochemical and mechanical environment cooperatively regulate skeletal muscle regeneration. *FASEB J.* **26,** 2538–2545
7. Landolt, R. M., Vaughan, L., Winterhalter, K. H., and Zimmermann, D. R. (1995) Versican is selectively expressed in embryonic tissues that act as barriers to neural crest cell migration and axon outgrowth. *Development* **121,** 2303–2312
8. Wu, Y. J., La Pierre, D. P., Wu, J., Yee, A. J., and Yang, B. B. (2005) The interaction of versican with its binding partners. *Cell Res.* **15,** 483–494
9. Knudson, C. B., and Toole, B. P. (1987) Hyaluronate-cell interactions during differentiation of chick embryo limb mesoderm. *Dev. Biol.* **124,** 82–90
10. Snow, H. E., Riccio, L. M., Mjaatvedt, C. H., Hoffman, S., and Capehart, A. A. (2005) Versican expression during skeletal/joint morphogenesis and patterning of muscle and nerve in the embryonic mouse limb. *Anat. Rec. A Discov. Mol. Cell Evol. Biol.* **282,** 95–105
11. Ermakova, I. I., Sakuta, G. A., Potekhina, M. A., Fedorova, M. A., Hoffmann, R., and Morozov, V. I. (2011) Major chondroitin sulfate proteoglycans identified in L6J1 myoblast culture. *Biochemistry* **76,** 359–365
12. Sandy, J. D., Westling, J., Kenagy, R. D., Iruela-Arispe, M. L., Verscharen, C., Rodriguez-Mazaneque, J. C., Zimmermann, D. R., Lemire, J. M., Fischer, J. W., Wight, T. N., and Clowes, A. W. (2001) Versican V1 proteolysis in human aorta *in vivo* occurs at the $Glu^{441}$-$Ala^{442}$ bond, a site that is cleaved by recombinant ADAMTS-1 and ADAMTS-4. *J. Biol. Chem.* **276,** 13372–13378
13. Apte, S. S. (2009) A disintegrin-like and metalloprotease (reprolysin-type) with thrombospondin type 1 motif (ADAMTS) superfamily. Functions and mechanisms. *J. Biol. Chem.* **284,** 31493–31497
14. Kintakas, C., and McCulloch, D. R. (2011) Emerging roles for ADAMTS5 during development and disease. *Matrix Biol.* **30,** 311–317
15. McCulloch, D. R., Le Goff, C., Bhatt, S., Dixon, L. J., Sandy, J. D., and Apte, S. S. (2009) *Adamts5*, the gene encoding a proteoglycan-degrading metalloprotease, is expressed by specific cell lineages during mouse embryonic development and in adult tissues. *Gene Expr. Patterns* **9,** 314–323
16. Longpré, J. M., McCulloch, D. R., Koo, B. H., Alexander, J. P., Apte, S. S., and Leduc, R. (2009) Characterization of proADAMTS5 processing by proprotein convertases. *Int. J. Biochem. Cell Biol.* **41,** 1116–1126
17. Malfait, A. M., Arner, E. C., Song, R. H., Alston, J. T., Markosyan, S., Staten, N., Yang, Z., Griggs, D. W., and Tortorella, M. D. (2008) Proprotein convertase activation of aggrecanases in cartilage *in situ*. *Arch. Biochem. Biophys.* **478,** 43–51
18. Glasson, S. S., Askew, R., Sheppard, B., Carito, B., Blanchet, T., Ma, H. L., Flannery, C. R., Peluso, D., Kanki, K., Yang, Z., Majumdar, M. K., and Morris, E. A. (2005) Deletion of active ADAMTS5 prevents cartilage degradation in a murine model of osteoarthritis. *Nature* **434,** 644–648
19. Stanton, H., Rogerson, F. M., East, C. J., Golub, S. B., Lawlor, K. E., Meeker, C. T., Little, C. B., Last, K., Farmer, P. J., Campbell, I. K., Fourie, A. M., and Fosang, A. J. (2005) ADAMTS5 is the major aggrecanase in mouse cartilage *in vivo* and *in vitro*. *Nature* **434,** 648–652
20. McCulloch, D. R., Nelson, C. M., Dixon, L. J., Silver, D. L., Wylie, J. D., Lindner, V., Sasaki, T., Cooley, M. A., Argraves, W. S., and Apte, S. S. (2009) ADAMTS metalloproteases generate active versican fragments that regulate interdigital web regression. *Dev. Cell* **17,** 687–698
21. McCulloch, D. R., Akl, P., Samaratunga, H., Herington, A. C., and Odorico, D. M. (2004) Expression of the disintegrin metalloprotease, ADAM-10, in prostate cancer and its regulation by dihydrotestosterone, insulin-like growth factor I, and epidermal growth factor in the prostate cancer cell model LNCaP. *Clin. Cancer Res.* **10,** 314–323
22. McCulloch, D. R., Wylie, J. D., Longpre, J. M., Leduc, R., and Apte, S. S. (2010) 10 mM Glucosamine prevents activation of proADAMTS5 (aggrecanase-2) in transfected cells by interference with post-translational modification of furin. *Osteoarthritis Cartilage* **18,** 455–463
23. Koo, B. H., Longpré, J. M., Somerville, R. P., Alexander, J. P., Leduc, R., and Apte, S. S. (2007) Regulation of ADAMTS9 secretion and enzymatic activity by its propeptide. *J. Biol. Chem.* **282,** 16146–16154
24. Horsley, V., Jansen, K. M., Mills, S. T., and Pavlath, G. K. (2003) IL-4 acts as a myoblast recruitment factor during mammalian muscle growth. *Cell* **113,** 483–494
25. Jansen, K. M., and Pavlath, G. K. (2006) Mannose receptor regulates myoblast motility and muscle growth. *J. Cell Biol.* **174,** 403–413
26. Park, I. H., and Chen, J. (2005) Mammalian target of rapamycin (mTOR) signaling is required for a late-stage fusion process during skeletal myotube maturation. *J. Biol. Chem.* **280,** 32009–32017
27. Hattori, N., Carrino, D. A., Lauer, M. E., Vasanji, A., Wylie, J. D., Nelson, C. M., and Apte, S. S. (2011) Pericellular versican regulates the fibroblast-myofibroblast transition. A role for ADAMTS5 protease-mediated proteolysis. *J. Biol. Chem.* **286,** 34298–34310
28. Brown, H. M., Dunning, K. R., Robker, R. L., Pritchard, M., and Russell, D. L. (2006) Requirement for ADAMTS-1 in extracellular matrix remodeling during ovarian folliculogenesis and lymphangiogenesis. *Dev. Biol.* **300,** 699–709
29. Somerville, R. P., Longpre, J. M., Jungers, K. A., Engle, J. M., Ross, M., Evanko, S., Wight, T. N., Leduc, R., and Apte, S. S. (2003) Characterization of ADAMTS-9 and ADAMTS-20 as a distinct ADAMTS subfamily related to *Caenorhabditis elegans* GON-1. *J. Biol. Chem.* **278,** 9503–9513
30. White, R. B., Biérinx, A. S., Gnocchi, V. F., and Zammit, P. S. (2010) Dynamics of muscle fiber growth during postnatal mouse development. *BMC Dev. Biol.* **10,** 21
31. Bains, W., Ponte, P., Blau, H., and Kedes, L. (1984) Cardiac actin is the major actin gene product in skeletal muscle cell differentiation *in vitro*. *Mol. Cell Biol.* **4,** 1449–1453
32. Orkin, R. W., Knudson, W., and Toole, B. P. (1985) Loss of hyaluronate-dependent coat during myoblast fusion. *Dev. Biol.* **107,** 527–530
33. Raganathan, S., and Datta, K. (1995) Presence of hyaluronan binding protein in cardiac myoblasts and its altered level during myogenesis. *Cell Biol. Int.* **19,** 161–165
34. Carrino, D. A., Sorrell, J. M., and Caplan, A. I. (1999) Dynamic expression of proteoglycans during chicken skeletal muscle development and maturation. *Poult. Sci.* **78,** 769–777
35. Jungers, K. A., Le Goff, C., Somerville, R. P., and Apte, S. S. (2005) Adamts9 is widely expressed during mouse embryo development. *Gene Expr. Patterns* **5,** 609–617
36. Stewart, M. C., Fosang, A. J., Bai, Y., Osborn, B., Plaas, A., and Sandy, J. D. (2006) ADAMTS5-mediated aggrecanolysis in murine epiphyseal chondrocyte cultures. *Osteoarthritis Cartilage* **14,** 392–402
37. Demircan, K., Hirohata, S., Nishida, K., Hatipoglu, O. F., Oohashi, T., Yonezawa, T., Apte, S. S., and Ninomiya, Y. (2005) ADAMTS-9 is synergistically induced by interleukin-1$\beta$ and tumor necrosis factor $\alpha$ in OUMS-27 chondrosarcoma cells and in human chondrocytes. *Arthritis Rheum.* **52,** 1451–1460
38. Velleman, S. G., Sporer, K. R., Ernst, C. W., Reed, K. M., and Strasburg, G. M. (2012) Versican, matrix Gla protein, and death-associated protein

expression affect muscle satellite cell proliferation and differentiation. *Poult. Sci.* **91,** 1964–1973
39. Velasco, J., Li, J., DiPietro, L., Stepp, M. A., Sandy, J. D., and Plaas, A. (2011) Adamts5 deletion blocks murine dermal repair through CD44-mediated aggrecan accumulation and modulation of transforming growth factor $\beta$1 (TGF$\beta$1) signaling. *J. Biol. Chem.* **286,** 26016–26027
40. Kashiwagi, M., Tortorella, M., Nagase, H., and Brew, K. (2001) TIMP-3 is a potent inhibitor of aggrecanase 1 (ADAM-TS4) and aggrecanase 2 (ADAM-TS5). *J. Biol. Chem.* **276,** 12501–12504
41. Liu, H., Chen, S. E., Jin, B., Carson, J. A., Niu, A., Durham, W., Lai, J. Y., and Li, Y. P. (2010) TIMP3. A physiological regulator of adult myogenesis. *J. Cell Sci.* **123,** 2914–2921
42. Goldspink, G., and Ward, P. S. (1979) Changes in rodent muscle fibre types during postnatal growth, undernutrition and exercise. *J. Physiol.* **296,** 453–469
43. Dupuis, L. E., McCulloch, D. R., McGarity, J. D., Bahan, A., Wessels, A., Weber, D., Diminich, A. M., Nelson, C. M., Apte, S. S., and Kern, C. B. (2011) Altered versican cleavage in ADAMTS5-deficient mice. A novel etiology of myxomatous valve disease. *Dev. Biol.* **357,** 152–164
44. Enomoto, H., Nelson, C. M., Somerville, R. P., Mielke, K., Dixon, L. J., Powell, K., and Apte, S. S. (2010) Cooperation of two ADAMTS metalloproteases in closure of the mouse palate identifies a requirement for versican proteolysis in regulating palatal mesenchyme proliferation. *Development* **137,** 4029–4038
45. Mittaz, L., Russell, D. L., Wilson, T., Brasted, M., Tkalcevic, J., Salamonsen, L. A., Hertzog, P. J., and Pritchard, M. A. (2004) Adamts-1 is essential for the development and function of the urogenital system. *Biol. Reprod.* **70,** 1096–1105
46. Russell, D. L., Doyle, K. M., Ochsner, S. A., Sandy, J. D., and Richards, J. S. (2003) Processing and localization of ADAMTS-1 and proteolytic cleavage of versican during cumulus matrix expansion and ovulation. *J. Biol. Chem.* **278,** 42330–42339
47. Rogerson, F. M., Stanton, H., East, C. J., Golub, S. B., Tutolo, L., Farmer, P. J., and Fosang, A. J. (2008) Evidence of a novel aggrecan-degrading activity in cartilage. Studies of mice deficient in both ADAMTS-4 and ADAMTS-5. *Arthritis Rheum.* **58,** 1664–1673
48. Tajbakhsh, S. (2009) Skeletal muscle stem cells in developmental versus regenerative myogenesis. *J. Internal. Med.* **266,** 372–389